Mon. Not. R. Astron. Soc. **000**, 000–000 (0000) Printed 11 January 1999 (MN LaTeX style file v1.4)

BeppoSAX Observations of 2-Jy Lobe-dominated Broad-Line Sources. I. The Discovery of a Hard X-ray Component

Paolo Padovani[1,2,3,⋆], Raffaella Morganti[4], Joachim Siebert[5], Fausto Vagnetti[3], Andrea Cimatti[6]

[1] *Space Telescope Science Institute, 3700 San Martin Drive, Baltimore MD. 21218, USA*
[2] *Affiliated to the Astrophysics Division, Space Science Department, European Space Agency*
[3] *Dipartimento di Fisica, II Università di Roma "Tor Vergata", Via della Ricerca Scientifica 1, I-00133 Roma, Italy*
[4] *Istituto di Radioastronomia, Via Gobetti 101, I-40129 Bologna, Italy*
[5] *Max-Planck-Institut für Extraterrestrische Physik, Giessenbachstrasse, D-85740 Garching bei München, Germany*
[6] *Osservatorio Astrofisico di Arcetri, Largo E. Fermi 5, I-50125 Firenze, Italy*

Accepted , Received

ABSTRACT

We present new *BeppoSAX* LECS, MECS and PDS observations of five lobe-dominated, broad-line active galactic nuclei selected from the 2-Jy sample of southern radio sources. These include three radio quasars and two broad-line radio galaxies. ROSAT PSPC data, available for all the objects, are also used to better constrain the spectral shape in the soft X-ray band. The collected data cover the energy range $0.1-10$ keV, reaching ~ 50 keV for one source (Pictor A). The main result from the spectral fits is that *all* sources have a hard X-ray spectrum with energy index $\alpha_{\rm x} \sim 0.75$ in the $2-10$ keV range. This is at variance with the situation at lower energies where these sources exhibit steeper spectra. Spectral breaks $\Delta\alpha_{\rm x} \sim 0.5$ at $1-2$ keV characterize in fact the overall X-ray spectra of our objects. The flat, high-energy slope is very similar to that displayed by flat-spectrum/core-dominated quasars, which suggests that the same emission mechanism (most likely inverse Compton) produces the hard X-ray spectra in both classes. Finally, a (weak) thermal component is also present at low energies in the two broad-line radio galaxies included in our study.

Key words: galaxies: active – X-ray: observations

1 INTRODUCTION

There is abundant evidence that strong anisotropies play a major role in the observed characteristics of radio loud active galactic nuclei (AGN; see Antonucci 1993 and Urry & Padovani 1995 for a review). Radio jets are in fact known to be strongly affected by relativistic beaming, while part of the optical emission in some classes of objects is likely to be absorbed by a thick disk or torus around the active nucleus.

A unification of all high-power radio sources has been suggested (Barthel 1989; Urry & Padovani 1995 and references therein) and according to this scheme, the lobe-dominated, steep-spectrum radio quasars (SSRQ) and the core-dominated, flat-spectrum radio quasars (FSRQ) are believed to be increasingly aligned versions of Fanaroff-Riley type II (FR II; Fanaroff & Riley 1974) radio galaxies. Within this scheme, broad-line (FWHM $\gtrsim$ 2000 km s^{-1}) radio galaxies (BLRG) have a still uncertain place. They could represent either objects intermediate between quasars and radio galaxies, (i.e., with the nucleus only partly obscured and the broad emission lines just becoming visible at the edge of the obscuring torus) or low-redshift, low-power equivalent of quasars.

The scenario described above makes a number of predictions about the X-ray emission of these radio-loud AGN. Moreover, the hard X-ray band, that is less affected by absorption, is essential for a complete knowledge of the intrinsic nature of these objects.

Although the X-ray spectrum can be very complex, the presence of a nuclear, likely beamed X-ray component in quasars is quite well established in particular for FSRQ and blazars (Wilkes & Elvis 1987; Shastri et al. 1993; Sambruna et al. 1994). There are mainly two arguments to support this: 1) the tendency for radio loud AGN to have systematically flatter X-ray slopes than radio quiet ones; 2) the fact that the soft X-ray slope decreases with core dominance (Shastri et al. 1993) and increases with radio spectral index (Fiore

⋆ Email: padovani@stsci.edu

et al. 1998). Both these results are explained with the presence of a radio-linked synchrotron self-Compton component of the X-ray emission that is likely to be beamed. This component would be dominant in the FSRQ. In SSRQ, in which "blazar-like", non-thermal emission is probably less important because of the larger angle w.r.t. the line of sight, the "UV bump" would be stronger (as effectively observed: e.g., Wills et al. 1995) and the steeper soft X-ray component would represent its high-energy tail.

Although a nuclear X-ray component has been detected also in radio galaxies, it appears to be much weaker than in radio quasars (consistent with the idea that radio galaxies have an obscured nucleus). For example, the X-ray spectrum of Cygnus A (Ueno et al. 1994) is consistent with a typical quasar spectrum absorbed by a high column density of cold gas along the line of sight. On the other hand, in the case of the broad-line radio galaxy 3C 390.3 (Inda et al. 1994), its hard X-ray spectrum can be described by a relatively flat, unabsorbed power-law. This would suggest that BLRG might well be the low-redshift counterpart of radio quasars and therefore aligned within $\lesssim 40^\circ$ (as predicted by unified schemes: see e.g., Urry & Padovani 1995).

From the above it is clear that a spectral X-ray study of lobe-dominated, broad-line radio sources (including both SSRQ and BLRG), covering a large X-ray band is necessary for a number of reasons. Namely: 1) to study the hard X-ray properties of lobe-dominated, broad-line radio sources, at present not well known; 2) to investigate if the difference in the soft X-ray spectra of SSRQ and FSRQ apply also to the hard X-ray band. The detection of a flatter component in SSRQ will be extremely important for our understanding of the emission processes in this class of objects; 3) to increase the number of BLRG for which the X-ray spectrum is known in detail in order to disentangle the real nature of BLRG and investigate if the X-ray spectra of BLRG and SSRQ are similar.

In this paper we present *BeppoSAX* observations of five lobe-dominated, broad-line radio sources, namely three SSRQ and two BLRG (we follow the commonly adopted definition of lobe-dominated source, which implies a value of the core dominance parameter $R < 1$). The sample is well defined (i.e., it is not a compilation of known hard X-ray sources) and it is extracted from the 2-Jy sample of radio sources for which a wealth of radio and optical information is available. The unique capability of the *BeppoSAX* satellite (Boella et al. 1997a) of performing simultaneous broad-band X-ray (0.1 – 200 keV) studies is particularly well suited for a detailed analysis of the X-ray energy spectrum of these sources.

In § 2 we present our sample, § 3 discusses the observations and the data analysis, while § 4 describes the results of our spectral fits to the *BeppoSAX* data. In § 5 we also examine the ROSAT PSPC data of our sources to better constrain the fits at low energies, in § 6 we combine the analysis of the *BeppoSAX* and ROSAT data while in § 7 we briefly comment on the lack of iron lines in our spectra. Finally, § 8 discusses our results and § 9 summarizes our conclusions. Throughout this paper spectral indices are written $S_\nu \propto \nu^{-\alpha}$.

2 THE SAMPLE

The lobe-dominated, broad-line objects studied in this paper belong to a complete subsample of the 2 Jy catalogue of radio sources (Wall & Peacock 1985). This subsample, defined by redshift $z < 0.7$ and declination $\delta < 10^\circ$, includes 88 objects and is complete down to a flux density level of 2 Jy at 2.7 GHz. Optical spectra are available for all the sources together with accurate measurements of the [O III]λ5007, [O II]λ3727 and Hβ emission line fluxes (Tadhunter et al. 1993, 1998). Estimates of the core dominance parameter R [$R = S_{core}/(S_{tot} - S_{core})$] have been derived from both arcsec-resolution images and higher resolution data (Morganti et al. 1993, 1997). A study of the soft X-ray characteristics of the objects in the sample has been carried out using the ROSAT All-Sky Survey and/or ROSAT PSPC pointed observations (Siebert et al. 1996). For most of the objects, however, no useful X-ray spectral information is available.

The 2 Jy subsample described above contains 16 lobe-dominated, broad-line objects (excluding compact steep-spectrum sources, whose relation to other classes is still not clear). From those, we have selected the 10 sources with estimated flux in the 0.1 – 10 keV band larger than 2×10^{-12} erg cm^{-2} s^{-1} for an X-ray spectral study with the *BeppoSAX* satellite[†]. Here we present the results obtained for the 5 objects so far observed in Cycle 1. The list of objects and their basic characteristics are given in Table 1, which presents the source name, position, redshift, optical magnitude V, 2.7 GHz radio flux, radio spectral index $\alpha_{\rm r}$ (taken from Wall & Peacock 1985), core dominance parameter R at 2.3 GHz, Galactic N_H and classification.

3 OBSERVATIONS AND DATA ANALYSIS

A complete description of the *BeppoSAX* mission is given by Boella et al. (1997a). The relevant instruments for our observations are the coaligned Narrow Field Instruments (NFI), which include one Low Energy Concentrator Spectrometer (LECS; Parmar et al. 1997) sensitive in the 0.1 – 10 keV band; three identical Medium Energy Concentrator Spectrometers (MECS; Boella et al. 1997b), covering the 1.5 – 10 keV band; and the Phoswich Detector System (PDS; Frontera et al. 1997), coaligned with the LECS and the MECS. The PDS instrument is made up of four units, and was operated in collimator rocking mode, with a pair of units pointing at the source and the other pair pointing at the background, the two pairs switching on and off source every 96 seconds. The net source spectra have been obtained by subtracting the 'off' to the 'on' counts. A journal of the observations is given in Table 2.

The data analysis was based on the linearized, cleaned event files obtained from the *BeppoSAX* Science Data Center (SDC) on-line archive (Giommi & Fiore 1997) and on the XIMAGE package (Giommi et al. 1991) upgraded to support the analysis of *BeppoSAX* data. The data from the

[†] Note that, as expected in any flux-limited sample, the 10 selected objects are ~ 30 times more luminous in the X-ray band than the 6 sources which did not make the X-ray flux cut. Our sample is then biased towards the most X-ray luminous lobe-dominated, broad-line sources in the 2-Jy sample.

Table 1. Sample Properties

Name	RA(J2000)	Dec(J2000)	z	V	$F_{2.7GHz}$ Jy	$\alpha_{2.7-5\ GHz}$	$R_{2.3GHz}$	Galactic N_H 10^{20} cm^{-2}	Class
OF −109	04 07 48.4	−12 11 36	0.574	14.9	2.35	0.42	0.57	3.81	QSO
Pictor A	05 19 49.0	−45 46 46	0.035	15.8	29.00	1.07	0.03	4.15	BLRG
OM −161	11 39 10.6	−13 50 43	0.554	16.2	2.80	0.65	0.16	3.59	QSO
PHL 1657	21 37 44.1	−14 32 55	0.200	15.5	2.00	0.63	0.06	4.45	QSO
PKS 2152−69	21 57 05.7	−69 41 23	0.027	13.8	19.27	0.71	0.03	2.50	BLRG

three MECS instruments were merged in one single event file by SDC. The LECS data above 4 keV were not used due to calibration uncertainties in this band that have not been completely solved at this time (Orr et al. 1998). As recommended by the SDC, LECS data have been then fitted only in the $0.1-4$ keV range, while MECS data were fitted in the $1.8-10.5$ keV range.

Spectra were accumulated for each observation using the SAXSELECT tool, with 8.5 and 4 arcmin extraction radii for the LECS and MECS respectively, which include more than 90% of the flux. The count rates given in Table 2 were obtained using XIMAGE and refer to channels 10 to 950 for the LECS and 36 to 220 for the MECS. The *BeppoSAX* images were also checked for the presence of serendipitous sources which could affect the data analysis. The ROSAT public images of our sources were also inspected (see below). Most of our objects have at least one source within the LECS extraction radius in the ROSAT PSPC and/or MECS images but at a flux level which is at maximum 10% of the target (and in most cases below 3%). Serendipitous sources in the field are then unlikely to affect our results at a significant level. We also looked for variability on timescales of 500 and 1,000 seconds for each observation, with null results.

The LECS and MECS background is low, although not uniformly distributed across the detectors, and rather stable. For this reason, and in particular for the spectral analysis, it is better to evaluate the background from blank fields, rather than in annuli around the source. Background files accumulated from blank fields, obtained from the SDC public ftp site, were then used.

4 SPECTRAL FITS

Spectral analysis was performed with the XSPEC 9.00 package, using the response matrices released by SDC in early 1997. The spectra were rebinned such that each new bin contains at least 20 counts (using the command GRPPHA within FTOOLS). Various checks using some of the rebinning files provided by SDC have shown that our results are independent of the adopted rebinning within the uncertainties. The X-ray spectra of our sources are shown in Figure 1 (which includes both *BeppoSAX* and ROSAT data: see Sect. 6).

4.1 LECS Data: Constraining N_H

At first, we fitted the LECS data with a single power-law model with Galactic and free absorption. The absorbing column was parameterized in terms of N_H, the HI column density, with heavier elements fixed at solar abundances. Cross sections were taken from Morrison and McCammon (1983). For one set of fits N_H was fixed at the Galactic value, derived from Elvis, Lockman & Wilkes (1989) for PHL 1657 and from the `nh` program at HEASARC (based on Dickey & Lockman 1990), for the remaining objects. N_H was also set free to vary to check for internal absorption and/or indications of a "soft-excess."

Our results are presented in Table 3, which gives the name of the source in column (1), the energy index α_x and reduced chi-squared and number of degrees of freedom, χ^2_ν(dof), in columns (2)-(3) for the fixed-N_H fits; columns (4)-(6) give N_H, α_x and χ^2_ν(dof) for the free-N_H fits. Finally, in column (7) we report the unabsorbed X-ray flux in the $0.1-4.0$ keV range (multiplied by a normalization constant derived from the combined LECS plus MECS fits: see next section). The errors quoted on the fit parameters are the 90% uncertainties for one and two interesting parameters for Galactic and free N_H respectively.

Two results are immediately apparent from Table 3: the fitted energy indices are flat ($\alpha_x < 1$); and the fitted N_H values are consistent with the Galactic ones. This is confirmed by an F-test which shows that the addition of N_H as a free parameter does not result in a significant improvement in the χ^2 values. We will then assume Galactic N_H in the combined LECS and MECS fits. For the two objects without LECS data this assumption is also justified by the fact that the fit to the MECS data is not strongly dependent on N_H.

The spectrum of PHL 1657 is more complicated than a simple power-law: the residuals show a clear excess at $E \lesssim 0.7$ keV. Indeed a broken power-law model significantly improves the fit (see below). Weaker "soft-excesses" cannot be excluded in the two other sources (see below) so the fluxes given in Table 3, based on a single power-law fit to the data, are almost certainly underestimated.

4.2 LECS and MECS Data

Our results from the jointly fitted LECS and MECS data assuming a single power-law model with Galactic absorption are presented in Table 4, which gives the name of the source in column (1), α_x and χ^2_ν(dof) in columns (2)-(3), and the unabsorbed X-ray flux in the $2-10$ keV range in column (4). The errors quoted on α_x are 90% uncertainties.

Due to the uncertainties in the calibration of the LECS instrument, the LECS/MECS normalization has been let free to vary. The resulting values, in the $0.6-0.8$ range, are consistent with the expected one (Giommi & Fiore, private communication).

The striking result is that *all* the sources have relatively flat X-ray energy indices. The mean value is $\langle\alpha_x\rangle = 0.75 \pm 0.02$ (here and in the following we give the standard deviation of the mean). This implies that the spectra are

Table 2. Journal of observations

Name	LECS exposure (s)	LECS count rate (10^{-2} s^{-1})	MECS exposure (s)	MECS count rate (10^{-2} s^{-1})	Observing date
OF −109	...	...	16,864	7.8 ± 0.3	22-SEP-1996
Pictor A	5,271	16.5 ± 0.7	14,798	26.4 ± 0.5	12/13-OCT-1996
OM −161	13,782	3.3 ± 0.2	28,248	5.7 ± 0.2	11/12-JAN-1997
PHL 1657	4,704	9.3 ± 0.6	17,429	18.0 ± 0.4	29-OCT-1996
PKS 2152−69	...	...	9,367	15.1 ± 0.5	29-SEP-1996

Table 3. LECS spectral fits

	Galactic	N_H	Free	N_H		
Name	α_x^a	χ^2_ν(dof)	N_H^b	α_x^b	χ^2_ν(dof)	Flux (0.1 – 4.0 keV)^c
			10^{20} cm^{-2}			10^{-12} erg cm^{-2} s^{-1}
Pictor A	$0.69^{+0.14}_{-0.14}$	0.78(30)	$2.75^{+2.79}_{-1.55}$	$0.60^{+0.23}_{-0.22}$	0.75(29)	17.6 ± 0.7
OM −161	$0.77^{+0.20}_{-0.22}$	0.77(24)	$3.70^{+7.80}_{-2.46}$	$0.77^{+0.40}_{-0.36}$	0.80(23)	3.8 ± 0.2
PHL 1657^d	$0.83^{+0.23}_{-0.24}$	1.01(16)	$2.75^{+3.48}_{-1.98}$	$0.69^{+0.38}_{-0.36}$	0.97(15)	13.5 ± 0.9

^{a} Quoted errors correspond to 90% uncertainties for one interesting parameter.
^{b} Quoted errors correspond to 90% uncertainties for two interesting parameters.
^{c} Unabsorbed flux. 1 σ statistical errors for best-fit model (model uncertainties not included). LECS fluxes have been multiplied by a normalization constant derived from the combined LECS and MECS fits ($\sim 0.6^{-1} - 0.8^{-1}$: see text).
^{d} An F-test shows that a broken power-law model improves the fit at the 98.1% level. Best-fit parameters are (for Galactic N_H): $\alpha_S = 1.2$, $\alpha_H = 0.3$, $E_{\rm break} = 1.6$ keV, $\chi^2_\nu({\rm dof}) = 0.84(14)$.

still raising in a $\nu - f_\nu$ plot, and therefore that the peak of the X-ray emission in the *BeppoSAX* band is at $E > 10$ keV. Table 4 also reports (in the footnotes) the fits to the MECS data for the three sources with both LECS and MECS observations. The energy indices in the $1.8 - 10.5$ keV range have a mean value $\langle \alpha_x \rangle = 0.74 \pm 0.03$, basically the same as in the whole $0.1 - 10.5$ keV band.

As mentioned in the Introduction, the spectra of the class of sources under study are generally steep at lower X-ray energies (and there is indeed strong evidence for a steeper X-ray component in the LECS data of PHL 1657). We then tried to fit a broken power-law model to our data. A significant improvement in the fit (96.5% level) was obtained only for PHL 1657, whose residuals again showed a clear excess at $E \lesssim 0.7$ keV. The best-fit parameters are $\alpha_S = 1.3$, $\alpha_H = 0.76 \pm 0.12$, and $E_{\rm break} = 0.9$ keV.

The fact that the other four sources show no significant evidence for a concave spectrum needs to be investigated with more data at soft X-ray energies. Hence the need to resort to ROSAT PSPC data (see Sect. 5).

4.3 The PDS Detection of Pictor A

Only the brightest source of our sample, Pictor A, has been detected by the PDS instrument (up to ~ 50 keV; see Fig. 1) despite the relative short exposure time (6.8 ks). The count rate is 0.18 ± 0.05 ct/s, that is the significance of the detection is about 3.6 σ. Given the relatively small statistics, it is hard to constrain the high energy ($E \gtrsim 10$ keV) spectrum of Pictor A. A parametrization of the MECS and PDS data with a single power-law model gives a best fit value of α_x perfectly consistent with that derived from MECS data only. A broken power-law model, with the soft energy index fixed to the value obtained from the MECS data (see Table 4), gives no significant improvement in the fit (and the hard energy index is consistent with the soft one). Therefore, the PDS data appear to lie on the extrapolation of the lower energy data. There might be a slight excess in the residuals above 10 keV but as described above this is not significant and does not warrant more complicated models.

5 ROSAT PSPC DATA

All our objects were found to have ROSAT PSPC data: namely, OF −109, Pictor A, PHL 1657 and PKS 2152−69 were all targets of ROSAT observations, while data for OM −161 were extracted from the ROSAT All-Sky Survey.

5.1 Data Analysis

In the analysis of the pointed PSPC observations, we first determined the centroid X-ray position by fitting a two-dimensional Gaussian to the X-ray image. Source counts were then extracted from a circular region with 3 arcmin radius around the centroid source position. The local background was determined from an annulus with inner radius 5 arcmin and outer radius 8 arcmin. If any X-ray sources were detected in the background region, they were first subtracted from the data.

The source counts from OM −161 were extracted from a circular region with radius 5 arcmin from the All-Sky Survey data. The larger extraction radius compared to the pointed PSPC observations accounts for the larger point spread function in the Survey. The local background was determined from two source-free regions with radius 5 arcmin, displaced from the source position along the scanning direction of the satellite during the All-Sky Survey.

After background subtraction, the data were vignetting and dead time corrected and finally binned into pulse height channels. Only channels 12-240 were used in the spectral analysis, due to existing calibration uncertainties at lower energies. The pulse height spectra were rebinned to achieve a constant signal-to-noise ratio in each spectral bin, which ranged from 3 to 6, depending on the total number of photons.

5.2 Spectral Fits

As for the LECS data, we fitted the ROSAT PSPC data with a single power-law model with Galactic and free absorption. Our results are presented in Table 5, which gives the name of the source in column (1), the ROSAT observation request

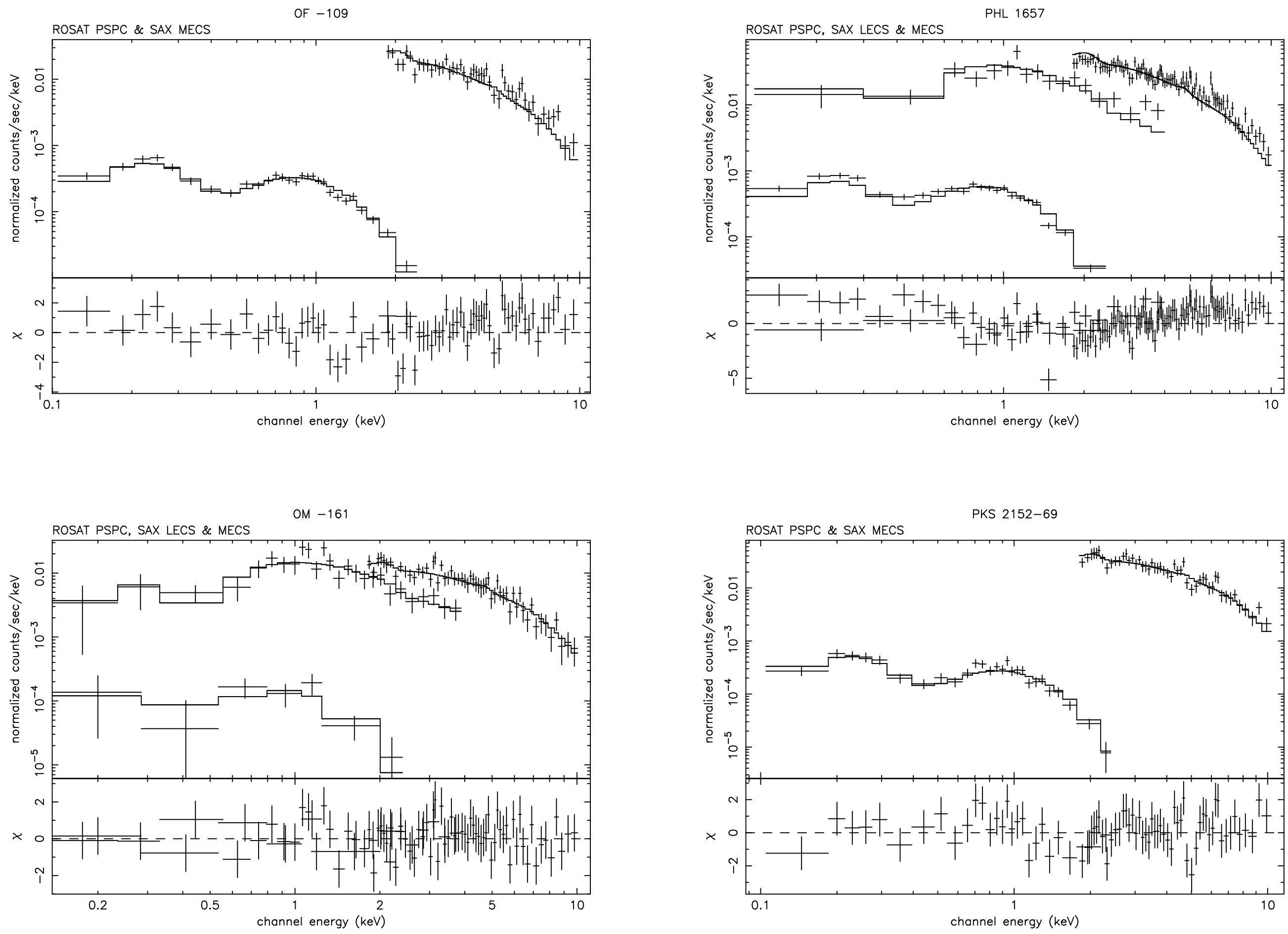

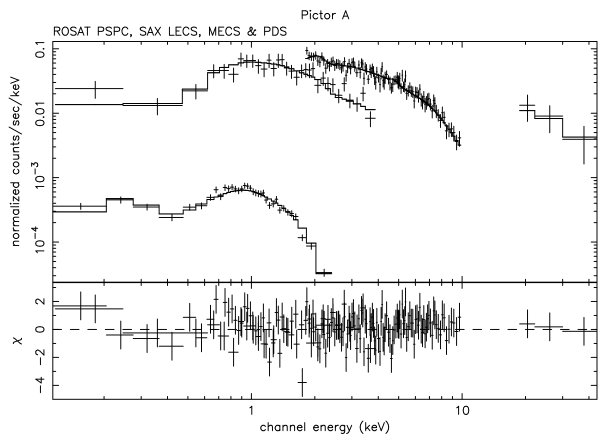

Figure 1. Spectra of the combined *BeppoSAX* and ROSAT PSPC data for our sources. The data are fitted with a single power-law model with Galactic absorption (free absorption for PKS 2152−69). Note that the ROSAT counts [lower spectra] have been normalized by the PSPC geometric area of 1,141 cm^2 and should be read as "normalized counts/sec/keV/cm^2."

Table 4. LECS and MECS spectral fits

Name	$\alpha_{\rm x}^a$	χ^2_ν(dof)	Flux (2 – 10 keV)[b] 10^{-12} erg cm^{-2} s^{-1}
OF −109[c]	$0.81^{+0.14}_{-0.14}$	1.17(46)	3.7 ± 0.1
Pictor A[d]	$0.68^{+0.06}_{-0.07}$	0.78(128)	13.8 ± 0.3
OM −161[e]	$0.77^{+0.11}_{-0.11}$	0.81(80)	2.5 ± 0.1
PHL 1657[f,g]	$0.78^{+0.08}_{-0.08}$	0.82(105)	8.6 ± 0.2
PKS 2152−69[c]	$0.70^{+0.12}_{-0.12}$	1.04(48)	7.5 ± 0.2

[a] Assuming Galactic N$_{\rm H}$.
[b] Unabsorbed flux. 1 σ statistical errors for best-fit model (model uncertainties not included).
[c] Only MECS data available.
[d] MECS only fit: $\alpha_{\rm x} = 0.67^{+0.07}_{-0.07}$, $\chi^2_\nu({\rm dof}) = 0.78(97)$
[e] MECS only fit: $\alpha_{\rm x} = 0.77^{+0.13}_{-0.12}$, $\chi^2_\nu({\rm dof}) = 0.84(55)$
[f] MECS only fit: $\alpha_{\rm x} = 0.77^{+0.08}_{-0.08}$, $\chi^2_\nu({\rm dof}) = 0.79(88)$
[g] An *F*-test shows that a broken power-law model improves the fit at the 96.5% level. Best-fit parameters are: $\alpha_{\rm S} = 1.3$, $\alpha_{\rm H} = 0.76 \pm 0.12$, $E_{\rm break} = 0.9$ keV, χ^2_ν(dof)= 0.81(103).

(ROR) number in column (2), $\alpha_{\rm x}$ and χ^2_ν(dof) in columns (3)-(4) for the fixed-N$_{\rm H}$ fits; columns (5)-(7) give N$_{\rm H}$, $\alpha_{\rm x}$ and χ^2_ν(dof) for the free-N$_{\rm H}$ fits. Finally, in column (8) we report the unabsorbed X-ray flux in the $0.1 - 2.4$ keV range. The errors quoted on the fit parameters are the 90% uncertainties for one and two interesting parameters for Galactic and free N$_{\rm H}$ respectively.

The main results of the ROSAT PSPC fits are the following: 1. the fitted energy indices are steeper than the

MECS (plus LECS) ones (with the exception of OM −161 for which the ROSAT α_x has large uncertainties); 2. there is no evidence for intervening absorption above the Galactic value in our sources, with the exception of PKS 2152−69, for which the F-test shows that the addition of N_H as a free parameter results in a significant improvement (98.6% level) in the goodness of the fit (the fitted N_H is about 50% higher than the Galactic value); 3. the single power-law fit is not great, although still acceptable, for Pictor A ($P_{\chi^2} \sim 5\%$) and PHL 1657 ($P_{\chi^2} \sim 7\%$).

The mean difference between the ROSAT PSPC and MECS (plus LECS) energy indices (excluding OM −161) is 0.44 ± 0.11, clearly indicative of a flattening at high energies, with the emergence of a hard component.

5.3 A Thermal Component in the X-ray Spectra of Pictor A and PKS 2152−69

Pictor A and PKS 2152−69 are relatively nearby objects ($z \leq 0.035$). The ROSAT PSPC images show evidence for an extended component on a scale $\gtrsim 50$" for PKS 2152−69 and $\gtrsim 70$" for Pictor A, which correspond to about 40 and 70 kpc respectively. PKS 2152-69 is also seen extended from ROSAT HRI data (Fosbury, private communication). Early-type galaxies are known to have diffuse emission from hot gas on these scales (Forman, Jones & Tucker 1985), so we added a thermal component (Raymond & Smith 1977) to the power-law model, assuming solar abundances (our results are only weakly dependent on the adopted abundances). Our results are reported in Table 6 which gives the name of the source in column (1), α_x in column (2), the gas temperature (in keV) in column (3), χ^2_ν(dof) in column (4), the ratio between the thermal and non-thermal components in the $0.1 - 2.4$ keV range in column (5), and finally the F-test probability in column (6). The errors quoted on the fit parameters are the 90% uncertainties for two interesting parameters. Galactic N_H as been assumed (see above). In both cases this addition results in a significantly improved fit (> 99.9% level) over a single power-law model. (Note that a Raymond-Smith model by itself gives extremely poor fits to the data.) With the addition of a thermal component the need for absorption above the Galactic value, which was indicated for PKS 2152−69 and suggested for Pictor A vanishes; free N_H fits now do not result in a significant improvement in the goodness of the fits.

As a check of our results we also fitted the spectra of OF −109 and PHL 1657 with a power-law plus thermal component. No need for an extra component was found, which is consistent with the fact that these two sources are at higher redshift (i.e., the putative thermal component is completely swamped by the stronger non-thermal emission).

It is interesting to note that the dominant component in the X-ray emission of our two nearest sources is definitely non-thermal, but nevertheless the data indicate a $5 - 10\%$ contribution from thermal emission. This is confirmed by an analysis of the PSPC images. The relevance of extended emission was in fact estimated by subtracting the point spread function (PSF) from the radial profile of the sources. For Pictor A, the fraction of photons above the PSF is 4%, while for PKS 2152−69 is 13% (for the two other sources with PSPC pointed data these fractions are less than 1%, as expected). Given the statistical and systematic uncertainties in the PSF (due to residual wobble motion, attitude uncertainties, etc.) these fractions agree very well with the results from the spectral decomposition (5 and 10% respectively).

The gas temperatures we find (< 1 keV) are very reasonable for gas associated with an elliptical galaxy (e.g., Forman et al. 1985). To check that the observed luminosities are also physically plausible, we performed the following test. There is a well-known strong correlation between X-ray luminosity and absolute blue magnitude for elliptical galaxies (e.g., Forman et al. 1985, 1994). Integrated blue magnitudes for Pictor A and PKS 2152−69, obtained from NED, imply $M_B \simeq -20.7$ and -22 respectively. The 0.5−4.5 keV luminosities for the thermal components of the two sources are $L_{0.5-4.5} \simeq 4 \times 10^{42}$ erg s^{-1} for Pictor A, with a rather large 90% error range ($10^{42} - 10^{43}$) while for PKS 2152−69 we get $L_{0.5-4.5} \simeq 2 \times 10^{42}$ erg s^{-1} (90% error range: $3 \times 10^{41} - 8 \times 10^{42}$). These numbers, compared against Fig. 4 of Forman et al. (1994), show that while the X-ray power in the thermal component of PKS 2152−69 is not unusual for its optical power, that of Pictor A is about an order of magnitude larger than the *maximum* values of elliptical galaxies of the same absolute magnitude. It then seems that the intrinsic power of the thermal component is too large to be associated with the galaxy.

As the relatively low gas temperature inferred from the data is also typical of small groups, one could speculate that most of the thermal emission in Pictor A is associated with a group associated with this source. An inspection of Fig. 8 of Ponman et al. (1996), which reports the X-ray luminosity – temperature relation for Hickson's groups, shows that, within the rather large errors, Pictor A might fall in the correct portion of the plot, although the best fit values ($L_x \simeq 4 \times 10^{42}$ erg s^{-1}, $kT = 0.55$ keV), would put it above the observed correlation. However, the richness of the environment of this source is very low (Zirbel 1997), inconsistent even with a small group. It might therefore be speculated that Pictor A is another example for a so-called fossil group (Ponman et al. 1994), i.e. a single elliptical galaxy that is considered to be the result of a merging process of a compact group. This merging is believed not to affect the X-ray halo of the group (Ponman & Bertram 1993) and the galaxies formed in this way will still show the extended thermal emission component of the intra-group gas although they appear isolated.

In summary, while the thermal component in PKS 2152−69 is consistent with emission from a hot corona around the galaxy, in the case of Pictor A the intrinsic power of this component is too high. However, the luminosity of the thermal component is consistent with that of a compact group of galaxies. Since Pictor A appears to be isolated, we might have another example of a fossil group.

We found no physically meaningful evidence for the presence of a thermal component in the LECS spectra of the three sources for which we have the relevant data.

6 ROSAT AND *BeppoSAX* DATA: THE WHOLE PICTURE

The last step is to put *BeppoSAX* and ROSAT PSPC data together to better constrain the shape of the X-ray spectra, especially at low energies. Two of our sources, in fact, have

Table 5. ROSAT PSPC spectral fits

Name	ROR #	Galactic α_x^a	N_H χ^2_ν(dof)	Free N_H^b 10^{20} cm^{-2}	N_H α_x^b	χ^2_ν(dof)	Flux (0.1 – 2.4 keV)^c 10^{-12} erg cm^{-2} s^{-1}
OF −109	701072	$1.30^{+0.07}_{-0.06}$	1.04(26)	$3.65^{+0.77}_{-0.72}$	$1.26^{+0.23}_{-0.23}$	1.08(25)	11.9 ± 0.3
Pictor A	700057	$0.80^{+0.05}_{-0.05}$	1.46(30)	$4.83^{+0.68}_{-0.65}$	$0.96^{+0.16}_{-0.17}$	1.34(29)^d	17.7 ± 0.3
OM −161	...	$0.80^{+0.55}_{-0.80}$	0.65(5)	6.2	1.3	0.73(4)^e	3.9 ± 0.8
PHL 1657	701542	$1.42^{+0.06}_{-0.05}$	1.49(20)	$4.86^{+0.75}_{-0.72}$	$1.53^{+0.22}_{-0.21}$	1.50(19)	23.7 ± 0.5
PKS 2152−69	701154	$0.86^{+0.09}_{-0.09}$	1.02(25)	$3.72^{+1.22}_{-1.10}$	$1.22^{+0.36}_{-0.35}$	0.83(24)^f	6.4 ± 0.2

[a] Quoted errors correspond to 90% uncertainties for one interesting parameter.
[b] Quoted errors correspond to 90% uncertainties for two interesting parameters.
[c] Unabsorbed flux. 1 σ statistical errors for best-fit model (model uncertainties not included).
[d] The reduction in the χ^2 value obtained with the free N_H fit is significant at the 93.7% level according to the F-test.
[e] The errors on the best-fit parameters are essentially undetermined due to the low photon statistics.
[f] The reduction in the χ^2 value obtained with the free N_H fit is significant at the 98.6% level according to the F-test.

Table 6. ROSAT PSPC spectral fits: thermal and non-thermal components

Name	α_x^a	kT^a keV	χ^2_ν(dof)	RS/power-law^b	P(F-test)^c
Pictor A	$0.79^{+0.08}_{-0.10}$	$0.55^{+0.40}_{-0.30}$	1.13(28)	0.05	99.97%
PKS 2152−69	$0.91^{+0.19}_{-0.19}$	$0.59^{+0.50}_{-0.37}$	0.73(23)	0.10	99.97%

[a] Quoted errors correspond to 90% uncertainties for two interesting parameters. Galactic N_H assumed.
[b] Flux ratio of the Raymond-Smith and power-law components in the $0.1 - 2.4$ keV band.
[c] Probability that the decrease in χ^2 due to the addition of the thermal component to the power-law model is significant.

no LECS data, while for the remaining three only less than 10 LECS bins are available below 1 keV. The ROSAT effective area is larger than the LECS effective area in the range of overlap, providing more leverage in the soft X-rays.

As before, we left free the LECS/MECS normalization and, as before, the fitted values are consistent with the expected ones. We also left free the PSPC/MECS normalization, to allow for any X-ray variability, which is seen in at least some lobe-dominated broad-line sources (e.g., 390.3: Leighly et al. 1997; 3C 382: Barr & Giommi 1992). However, the PSPC/MECS normalization was, on average, around 1, with a maximum excursion of 30−40%. No strong variability is then present between the ROSAT and *BeppoSAX* data.

As it turned out, in all cases for which we had enough statistics at low energies (i.e., excluding OM −161) a broken power-law model resulted in a significantly improved fit ($\geq$ 99.9% level) over a single power-law model over the whole 0.1 – 10.5 keV range. Our results are reported in Table 7 which gives the name of the source in column (1), α_S, α_H, and $E_{\rm break}$ in columns (2)-(4), χ^2_ν(dof) in column (5) and finally the F-test probability in column (6). The errors quoted on the fit parameters are the 90% uncertainties for three interesting parameters. Based on the LECS and ROSAT PSPC results, Galactic N_H as been assumed for all sources apart from PKS 2152−69. The combined data with the best fit single power-law model (to show the spectral concavity) are shown in Figure 1.

As can be seen from the Table, the model parameters are extremely well determined. Not surprisingly, the α_S values are very similar to the ROSAT PSPC energy indices, while the α_H values are basically the same as the MECS (plus LECS) energy indices. The spectra are obviously concave, with $\langle\alpha_S - \alpha_H\rangle = 0.49 \pm 0.09$ and energy breaks around 1.5 keV (Pictor A has a break at about 4 keV but with a large error due to the relatively small difference between the soft and the hard spectral indices). The fact that the breaks fall at relatively low energies explain why the energy indices derived from the LECS fits are basically the same as those obtained from the combined LECS and MECS fits.

The addition of a thermal component in Pictor A and PKS 2152−69 improves significantly the fit (> 99.8% level) even in the case of a broken power-law model. As for the single power-law plus thermal component, free N_H fits do not result in a significant improvement in the goodness of the fits, so Galactic N_H is assumed. Best-fit parameters are $\alpha_S = 0.77$, $\alpha_H = 0.66$, $E_{\rm break} = 2.1$ keV, $kT = 0.39$ keV, for Pictor A, and $\alpha_S = 0.92$, $\alpha_H = 0.68$, $E_{\rm break} = 1.4$ keV, $kT = 0.57$ keV, for PKS 2152−69. These are perfectly consistent with those obtained from the broken power-law fit to the *BeppoSAX* and ROSAT PSPC data and with the temperatures derived from the ROSAT PSPC data, but the uncertainties are now poorly determined because of the relatively large number of parameters.

7 IRON LINES?

A number of AGN exhibit in their X-ray spectra iron Kα lines which are characteristic of relativistic effects in an accretion disk surrounding a central black hole (e.g., Nandra & Pounds 1994). It appears that radio-loud AGN have weaker iron lines than radio-quiet ones, although some low-luminosity, radio-loud sources are known to have strong iron lines (Nandra et al. 1997).

We searched for Fe Kα emission in our MECS spectra: none was found. The 90% upper limits on the equivalent width (in the source rest frame) of an unresolved iron line ($\sigma = 0$) at energy 6.4 keV are the following: OF −109: 380 eV; Pictor A: 150 eV; OM −161: 300 eV; PHL 1657: 170 eV; PKS 2152−69: 400 eV. Note that for any broader line the limits are correspondingly higher. Our result for Pictor A is consistent with the upper limit of 100 eV given by Eracleous

Table 7. ROSAT PSPC, BeppoSAX LECS and MECS spectral fits

Name	$\alpha_{\rm S}^a$	$\alpha_{\rm H}^a$	$E^a_{\rm break}$ keV	χ^2_ν(dof)	P(F-test)[b]
OF −109	$1.33^{+0.11}_{-0.10}$	$0.80^{+0.20}_{-0.21}$	$1.32^{+1.39}_{-0.37}$	1.06(71)	>99.99%
Pictor A	$0.79^{+0.07}_{-0.07}$	$0.56^{+0.21}_{-0.38}$	$3.92^{+4.88}_{-3.10}$	0.91(157)	99.90%
OM −161	...	$0.77^{+0.11}_{-0.11}$	...	0.79(86)	...
PHL 1657	$1.42^{+0.09}_{-0.09}$	$0.75^{+0.12}_{-0.12}$	$1.45^{+0.50}_{-0.29}$	0.96(124)	>99.99%
PKS 2152−69[c]	$1.23^{+0.57}_{-0.41}$	$0.70^{+0.18}_{-0.18}$	$1.69^{+2.01}_{-0.75}$	0.98(71)	>99.99%

[a] Quoted errors correspond to 90% uncertainties for three interesting parameters for all sources apart from OM −161 (one interesting parameter). Galactic $N_{\rm H}$ assumed for all sources apart from PKS 2152−69.
[b] Probability that the decrease in χ^2 due to the addition of two parameters (from a single power-law fit to a broken power-law fit) is significant.
[c] Fit with free $N_{\rm H} = 3.8^{+1.0}_{-0.9} \times 10^{20}$ cm^{-2}.

& Halpern (1998) based on a $\sim$ 65 ks *ASCA* observation, and our limit for PHL 1657 agrees with the upper limit of 140 eV given by Williams et al. (1992) based on a 15 ks *Ginga* observation.

We note that the upper limits on iron lines in our sources are not very stringent and still consistent with values found in other lobe-dominated broad-lined sources (e.g., Inda et al. 1994; Lawson & Turner 1997; Woźniak et al. 1998).

8 DISCUSSION

We have presented the first systematic, hard X-ray study of a well-defined sample of lobe-dominated, broad-line AGN. Our main result is that this class of objects has a hard X-ray spectrum with $\alpha_{\rm x} \sim 0.75$ at $E \gtrsim 1-2$ keV. In addition, we also detect a thermal emission component present at low energies in the spectra of two BLRGs, but we find that this component contributes only $\lesssim 10\%$ of the total flux.

Hard X-ray emission is also present in core-dominated radio-loud quasars, and the detection of similarly flat spectra in our sample of lobe-dominated AGN has important implications for our understanding of the relation between the two classes.

In order to make a more quantitative comparison between the hard X-ray spectra of the two classes we searched the literature for a study of core-dominated/flat-spectrum radio quasars similar to ours, i.e., based on a well-defined, homogeneous sample. Surprisingly, we found none. We then decided to collect all the information we could find on the $2-10$ keV spectra of FSRQ, excluding objects with large (> 0.5) uncertainties on the X-ray spectral index. The data come from *Ginga* and EXOSAT/ME observations published in Makino (1989), Ohashi et al. (1989, 1992), Lawson et al. (1992), Saxton et al. (1993), Williams et al. (1992), Sambruna et al. (1994) and Lawson & Turner (1997; $\alpha_{\rm x}$ in the $2-18$ keV range). The resulting sample includes 15 objects and is characterized by $\langle\alpha_{\rm x}\rangle = 0.70 \pm 0.06$, perfectly consistent with our results.

We stress again that the sample of FSRQ is heterogeneous whereas our sample, although relatively small, is well defined and has very well determined spectral indices. However, within the limits introduced by the biases likely present in the FSRQ sample, lobe-dominated and core-dominated broad-line AGN appear to have practically identical hard X-ray spectra in the $2-10/18$ keV region.

The objects in our sample are lobe dominated and therefore we investigated if inverse Compton scattering of cosmic microwave background photons into the X-ray band by relativistic electrons in the diffuse radio lobes could be responsible for the observed X-ray emission (see e.g., Harris & Grindlay 1979; Feigelson et al. 1995). We find that this is not the case and the derived X-ray emission is almost two orders of magnitude lower than observed. This is further supported by the fact that no strong resolved components have been found for our objects by ROSAT. The hotspot in Pictor A is known to have associated X-ray emission but this is very weak and indeed only marginally detected by Einstein (Röser & Meisenheimer 1987; Perley et al. 1997).

The hard X-ray component present in FSRQ is usually interpreted as due to inverse Compton emission, most likely due to a combination of synchrotron self-Compton emission (with the same population of relativistic electrons producing the synchrotron radiation and then scattering them to higher energies) and Comptonization of external radiation (possibly emitted by material being accreted by the central object; see e.g., Sikora, Begelman & Rees 1994). As the hard X-ray emission in our sources has a similar, flat slope, it seems natural to attribute it to the same emission mechanism. The smaller effect of Doppler boosting for lobe dominated sources would then make this component to appear and become dominant only at high energies, and this is exactly what is shown by our data. This is further confirmed and clearly shown in Figure 2, where we plot the $2-10$ keV spectral index *versus* the core dominance parameter R. (The open triangles indicate the SSRQ and BLRG found in the literature, in some of the papers listed above for FSRQ). It is evident from the figure that no correlation is present between the two quantities. This seems in disagreement with the correlation claimed by Lawson et al. (1992) (based on EXOSAT/ME data) and Lawson & Turner (1997) (based on *Ginga* data), the only previous hard X-ray studies which included some steep-spectrum radio quasars. We note that the spectral indices derived from EXOSAT data had relatively large errors and that our sample of FSRQ, SSRQ and BLRG is larger than the samples used by Lawson et al. (1992) and Lawson & Turner (1997) (26 vs. 18 and 15 objects respectively) especially as far as lobe-dominated broad-line sources are concerned (where we have basically doubled the number of available sources). Moreover, the correlation claimed by Lawson & Turner (1997) becomes significant only by excluding the three BLRG in their sample (the exclusion of the BLRG has no effect on the lack of correlation between

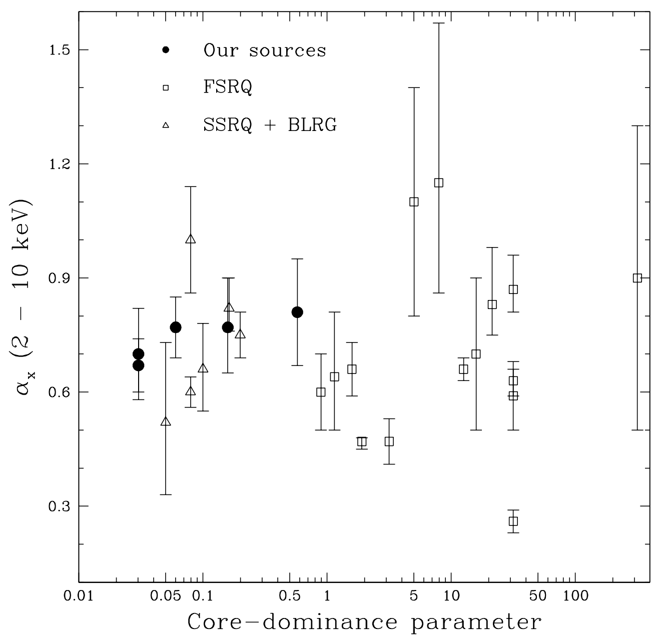

Figure 2. The $2-10$ keV ($2-18$ keV for 10 sources from Lawson & Turner 1997) X-ray spectral index versus the core-dominance parameter for our sources (filled symbols) and core-dominated flat-spectrum radio quasars (FSRQ: empty squares) and lobe-dominated steep-spectrum radio quasars and broad-line radio galaxies (SSRQ + BLRG: triangles) from the literature. Error bars represent 90% errors for our objects and 1 σ errors for most of the other sources. See text for details.

α_x and R in our sample). Larger homogeneous samples (especially of FSRQ) are clearly required in order to investigate this issue in more details.

Our hard X-ray spectra are well fitted by a single power law and we find no evidence for the hard excess often seen in low-luminosity AGN (e.g., Nandra & Pounds 1994) and interpreted as due to Compton reflection of the X-rays off optically thick material (Guilbert & Rees 1988; Lightman & White 1988). In the case of Pictor A, this is also confirmed by the results of Eracleous & Halpern (1998) based on a longer *ASCA* observation. We note, however, that this reflection component should normally be apparent above ~ 10 keV and that our data reach these energies only for Pictor A (and even then with relatively small statistics; see Sect. 4.3).

Woźniak et al. (1998) have recently studied the X-ray (and soft γ-ray) spectra of BLRG using *Ginga*, *ASCA*, OSSE and EXOSAT data. Their object list includes 4 lobe-dominated BLRG, namely 3C 111, 3C 382, 3C 390.3, and 3C 445. The X-ray spectra have an energy index $\alpha_x \sim 0.7$, with some moderate absorption. Fe Kα lines have also been detected with typical equivalent widths ~ 100 eV. Any Compton reflection component is constrained to be weak and is unambiguously detected only in 3C 390.3. Our results are consistent with their findings.

Our MECS results for PHL 1657 are in agreement with the *Ginga* energy slope obtained by Williams et al. (1992: see their Table 3), while our $2-10$ keV flux appears to be $\sim 35\%$ smaller. Eracleous & Halpern (1998) reported on a ~ 65 ks *ASCA* observations of Pictor A. Our LECS and MECS data appear to require a slightly flatter spectral index than given by these authors (0.77 ± 0.03, from the SIS and GIS fits) while our $2-10$ flux is similar to that derived from the SIS (but $\sim 10\%$ smaller than the $2-10$ keV flux estimated from the GIS).

As discussed in the Introduction, various previous studies had found that SSRQ displayed a steep soft X-ray spectrum (see, e.g., Fiore et al. 1998). In fact, despite the hard component at higher energies, we nevertheless observe a steeper spectrum at lower energies. In the whole ROSAT band we find $\alpha_x = 1.19 \pm 0.13$ (excluding OM−161, for which the ROSAT α_x has large uncertainties), which is intermediate between the values obtained for SSRQ by Fiore et al. (1998) between $0.4-2.4$ keV ($\alpha_x = 1.14$) and $0.1-0.8$ keV ($\alpha_x = 1.37$). Our best fits to the whole $0.1-10$ keV range indeed *require* a spectral break $\Delta\alpha_x \sim 0.5$ between the soft and hard energy slopes at about $1-2$ keV. The dispersion in the energy indices is larger for the soft component. We find $\sigma(\alpha_S) = 0.28$ while $\sigma(\alpha_H) = 0.10$, which might suggest a more homogeneous mechanism at higher energies. We note that Fiore et al. (1998) also found a concave spectrum ($\alpha_{0.1-0.8 \text{ keV}} - \alpha_{0.4-2.4 \ keV} \simeq 0.2$) for radio-loud AGN (both flat- and steep-spectrum) in the ROSAT band.

There are some concerns (R. Mushotzky, private communication) of miscalibration between ROSAT, on one side, and *BeppoSAX*, *ASCA* and RXTE on the other side, which could affect some of our conclusions. Namely, the inferred ROSAT spectral indices might be steeper than those derived, in the same band, by other X-ray satellites (a detailed comparison of simultaneous *ASCA*/RXTE/*BeppoSAX* spectra of 3C 273 is given by Yaqoob et al. in preparation). The spectral breaks we find in the spectra of our objects could then be partly due to this effect. This is clearly an important point, very relevant for X-ray astronomy, but which goes beyond the scope of this paper. Nevertheless, we can still comment on this as follows: 1. the "*BeppoSAX* only" spectrum of PHL 1657 shows, by itself, significant evidence of a break, with best fit parameters consistent (within the rather large errors) with those obtained from the full ROSAT and *BeppoSAX* fit (see Sect. 4.2). At least in this source, then, the evidence for a spectral break is "ROSAT independent." The fact that this is not the case for the two other objects with LECS data, Pictor A and OM−161, can be explained by the relatively smaller break in the first object and the small LECS statistics in the latter. In other words, the available evidence is *consistent* with breaks similar to those derived from the combined ROSAT and *BeppoSAX* fits to be present also in the LECS/MECS data; 2. our main result, that is, the presence of a hard X-ray component in all our sources at $E \gtrsim 1-2$ keV, is based on *BeppoSAX* data and therefore clearly independent of any possible ROSAT miscalibration.

One could also worry about possible miscalibrations between different X-ray instruments affecting the (lack of) correlation in Fig. 2. However, the results of Woźniak et al. (1998) appear to exclude that possibility. The *ASCA*, *Ginga* and EXOSAT X-ray spectra of the sources studied by these authors, in fact, agree within the errors, particularly in the hard X-ray band. Given the good cross-calibration between *BeppoSAX* and *ASCA*, a large miscalibration between *BeppoSAX*, *Ginga* and EXOSAT (the instruments used to obtain the data used in Fig. 2) seems to be ruled out.

9 CONCLUSIONS

The main conclusions of this paper, which presents *BeppoSAX* data for a well defined sample of 2-Jy steep-spectrum radio quasars and broad-line radio galaxies can be summarized as below.

All five lobe-dominated, broad-line sources included in this study have been clearly detected up to 10 keV (50 keV for Pictor A) and display a flat X-ray spectrum ($\alpha_{\rm x} \sim 0.75$) in the $2-10$ keV range. One source (out of the three with LECS and MECS data, i.e., reaching down to 0.1 keV) shows significant evidence of a spectral break at $E \sim 1$ keV. When ROSAT PSPC data, available for all five sources, are included in the fit, the evidence for concave overall spectra, with $\alpha_{\rm soft} - \alpha_{\rm hard} \sim 0.5$ and $E_{\rm break} \sim 1.5$ keV, becomes highly significant for all objects with good enough statistics at low energies (i.e., excluding OM$-$161). No iron lines are detected in our spectra but the upper limits we derive are not very stringent (due to the relatively short exposure times). The flat high-energy slope we find for our lobe-dominated sources is consistent with the hard X-ray emission present in core-dominated radio quasars. In fact, by collecting data from the literature on the X-ray spectra of radio quasars, we show that the available data are consistent with *no dependence* between the $2-10$ keV spectral indices and the core-dominance parameter, somewhat in contrast with the situation at lower energies. Finally, a thermal emission component is present at low energies in the spectra of the two broad-line radio galaxies, although only at the $\sim 10\%$ level.

Three more targets have been approved as part of this *BeppoSAX* observing program (one at a lower priority). We will be presenting results on these additional objects, and a more thorough discussion of the implications of our results in terms of emission processes, orientation, and more generally unified schemes in a future paper.

ACKNOWLEDGEMENTS

We acknowledge useful discussions with Alfonso Cavaliere, Andrea Comastri, Fabrizio Fiore, Paolo Giommi, Paola Grandi, Richard Mushotzky, Tahir Yaqoob. We thank Paola Grandi also for her help with the analysis of the PDS data of Pictor A. This research has made use of the NASA/IPAC Extragalactic Database (NED), which is operated by the Jet Propulsion Laboratory, California Institute of Technology, under contract with the National Aeronautics and Space Administration.

REFERENCES

Antonucci R., 1993, ARA&A, 31, 473
Baker J.C., Hunstead R.W., Brinkmann W., 1995, MNRAS, 277, 553
Barr P., Giommi P., 1992, MNRAS, 255, 495
Barthel P.D., 1989, ApJ, 336, 319
Boella G. et al., 1997a, A&AS, 122, 299
Boella G. et al., 1997b, A&AS, 122, 327
Dickey J.M., Lockman F.J., 1990, ARA&A, 28, 215
Elvis M., Lockman F.J., Wilkes B.J., 1989, AJ, 97, 777
Eracleous M., Halpern J.P., 1998, ApJ, in press (astro-ph/9805253)
Fanaroff B.L., Riley J.M., 1974, MNRAS, 167, 31P
Feigelson E.D., Laurent-Muehleisen S.A., Kollgaard R.I., 1995, ApJ, 449, L149
Fiore F., Elvis M., Giommi P., Padovani P., 1998, ApJ, 492, 79
Forman W., Jones C., Tucker A., 1985, ApJ, 293, 102
Forman W., Jones C., Tucker A., 1994, ApJ, 429, 77
Frontera F. et al., 1997, A&AS, 122, 357
Giommi P., Fiore F., 1997, in 5th International Workshop on Data Analysis in Astronomy, Erice, in press
Giommi P., Angelini L., Jacobs P., Tagliaferri G., 1991 in Worrall D.M., Biemesderfer C., Barnes J., eds, ASP Conf. Ser. Vol. 25, Astronomical Data Analysis Software and Systems I, Astrom. Soc. Pac., San Francisco, p. 100
Guilbert P.W., Rees M.J., 1988, MNRAS, 233, 475
Harris D.E., Grindlay J.E., 1979, MNRAS, 188, 25
Inda M. et al., 1994, ApJ, 420, 143
Lawson A.J., Turner M.J.L., 1997, MNRAS, 288, 920
Lawson A.J., Turner M.J.L., Williams O.R., Stewart G.C., Saxton R.D., 1992, MNRAS, 259, 743
Leighly K.M., O'Brien P.T., Edelson R., George I.M., Malkan M.A., Matsuoka M., Mushotzky R.F., Peterson B.M., 1997, ApJ, 483, 767
Lightman A.P., White T.R., 1988, ApJ, 335
McDowell J.C. et al., 1989, ApJ, 345, L13
Morganti R., Killeen N.E.B., Tadhunter C.N., 1993, MNRAS, 263, 1023
Morganti R., Oosterloo T.A., Reynolds J.E., Tadhunter C.N., Migenes V., 1997 MNRAS, 284, 541
Morrison R., McCammon D., 1983, ApJ, 270, 119
Nandra K., Pounds K.A., 1994, MNRAS, 268, 405
Nandra K., George I.M., Mushotzky R.F., Turner T.J., Yaqoob T., 1997, ApJ, 488, L91
Orr A., Parmar, A.N., Yaqoob T., Guainazzi M., 1998, in Scarsi L., Bradt H., Giommi P., Fiore F., eds, The Active X-ray Sky: Results from BeppoSAX and Rossi-XTE, Elsevier, Amsterdam, p. 497
Parmar A. et al., 1997, A&AS, 122, 309.
Perley R., Röser H.-J., Meisenheimer K., 1997, A&A, 328, 12
Ponman T.J., Betram D., 1993, Nature 363, 51
Ponman T.J, Allan D.J., Jones L.R., Merrifield M., McHardy I.M., Lehto H.J., Luppino G.A., 1994, Nature 369, 462
Ponman T.J., Bourner P.D.J., Ebeling H., Böhringer H., 1996, MNRAS, 283, 690
Raymond J.C., Smith B.W., 1977, ApJS, 35, 419
Röser H.-J., Meisenheimer K., 1987, ApJ, 314, 70
Sambruna R., Barr P., Giommi P., Maraschi L., Tagliaferri G., Treves A., 1994, ApJS, 95, 371
Saxton R.D., Turner M.J.L., Williams O.R., Stewart G.C., Ohashi T., Kii T., 1993, MNRAS, 262, 63
Shastri P., Wilkes B.J., Elvis M., McDowell J., 1993, ApJ, 410, 29
Siebert J., Brinkmann W., Morganti R., Tadhunter C.N., Danziger I.J., Fosbury R.A.E., di Serego Alighieri S., 1996, MNRAS, 279, 1331
Sikora M., Begelman M.C., Rees M.J., 1994, ApJ, 421, 153
Tadhunter C.N., Morganti R., di Serego Alighieri S., Fosbury R.A.E., Danziger I.J., 1993, MNRAS, 263, 999
Tadhunter C.N., Morganti R., Robinson A., Dickson R., Villar-Martin M., Fosbury R.A.E., 1998, MNRAS, 298, 1035
Ueno, S. et al., 1994, ApJ, 431, L1
Urry C.M., Padovani P., 1995, PASP, 107, 803
Wall J.V., Peacock, J.A., 1985, MNRAS, 216, 173
Wilkes B.J., Elvis M., 1987, ApJ, 323, 243
Williams O.R. et al., 1992, ApJ, 389, 157
Wills B.J. et al., 1995, ApJ, 447, 139
Worrall D.M., Giommi P., Tananbaum H., Zamorani G., 1987, ApJ, 313, 596
Woźniak P.R., Zdziarski A.A., Smith D., Madejski G.M., Johnson W.N., 1998, MNRAS, 299, 449

Zirbel E.L., 1997, ApJ, 476, 489